

Sludge Formation in Hall Héroult Process: An Existing Problem

Mojtaba Fallah Fini¹, Gervais Soucy², Martin Désilets³,
Patrick Pelletier⁴, Didier Lombard⁵ and Loig Rivoaland⁶

1. PhD student, 2. Professor, 3. Professor

Department of Chemical Engineering & Biotechnological Engineering,
Université de Sherbrooke, Sherbrooke, QC, Canada

4. Research Scientist, Rio Tinto, R&D Arvida Center, Jonquière, QC, Canada

5. Consultant, LRF, Rio Tinto, Saint Jean de Maurienne, France

6. Cathode Materials Expert, Carbone Savoie, Vénissieux, France

Corresponding author: Gervais.Soucy@usherbrooke.ca

Abstract

A concise literature review is done on the industrial and laboratory scale investigations of sludge formation in the Hall Héroult Process. Formation of sludge and consequently its transformation into resistive cathodic deposits has been one of the focal concerns of the aluminum producers. However, nowadays due to the profusion of production, especially by China, all the major producers of aluminum have increased their efforts towards sludge minimization and better understanding of the phenomena that lead to formation of such deposits. In this review article, first the sludge formation phenomenon and its detrimental effect in Hall-Héroult process is introduced. Later, the thermochemistry of the sludge is presented. Furthermore, four of the most important factors in sludge formation namely hydrodynamics, operational temperature (i.e. superheat level), alumina feeding and bath chemistry are reviewed.

Keywords: Hall Héroult process, hydrodynamics, sludge formation, alumina feeding strategy, bath chemistry and operational temperature.

1. Introduction

Aluminum is a strategic metal in transportation, packaging, construction, electrical industry, consumer durables and machinery [1]. Furthermore, recent developments in the production of aluminum batteries has created yet another potential market for the consumption of aluminum in the future [2]. According to the world's annual production of aluminum and its trend in recent years, China has become a formidable producer of aluminum in the last 6 years [3] and this has forced other producers of aluminum to try to reduce their production cost more and more by investing in research and development (R&D).

In an ideal aluminum electrolysis process, according to Faraday's law, 0.335573 kg of aluminum is produced with 1 kAh of electrical charge. However, in reality, a current efficiency of $\approx 95 - 96 \%$ is observed [4]. Two major phenomena account for such a loss of current efficiency. The first reason is the back reaction of solubilized aluminum ions with CO_2 gas and production of CO gas and dissolved Al_2O_3 . The second major phenomenon is the formation of resistive deposits on the surface of the cathode. Such deposits not only create more resistivity against the electrical current and increase the required electrical energy, but also as it is mentioned in the following paragraphs (Section 2.), contributes to the four significant factors reducing the current efficiency.

2. Sludge Formation and Its Drawbacks

In an ideal scenario, upon the introduction of alumina onto the cryolitic bath surface, alumina particles easily dissolve and disperse evenly at interelectrode space (i.e. distance between anode

and upper surface of metal pad). Unfortunately, just like most of engineering cases, such ideal situation is hardly possible and when undissolved clumps of alumina sink to the bottom of the cell, beneath the metal pad, a dense and viscous phase called sludge is formed. According to [Tabereaux and Peterson \[4\]](#), the following steps are followed upon addition of 1 – 2 kg of alumina particles onto the surface of bath by point feeders. At first, the particles get wetted by the bath. Later the alumina particles absorb the sensible heat and their temperature increases from 100 °C to 960 °C. At this stage, the wetted undissolved particles form agglomerates and subsequent dissolution occurs around the alumina particles creating a supersaturated local bath. Gradually most of the alumina particles dissolve into the bath and distribute in the cell by the turbulence flow. Sludge is a paste-like viscous combination of alumina particles and alumina-saturated bath. The average properties of a typical sludge sample is as follows: density of $\sim 2\,400\text{ kg/m}^3$, alumina content of 20 - 50 %, AlF_3 of 2 - 10 %, CaF_2 of 2 - 5 % [[5](#), [6](#): p. 77].

Formation of sludge is not a favorable phenomenon due to the fact that, it contributes to the four significant factors reducing the current efficiency, namely operational temperature, bath chemistry, current density and the stability of the metal-bath interface. A typical sludge phase with the aforementioned characteristics has an electrical resistivity of $0.01\ \Omega\text{m}$ [[7](#), [8](#)], which is about twice the resistivity of bath and about 35 000 times greater than molten aluminum. Such electrical resistivity diverts the local current density and creates areas with higher current density and consequently higher cathode wear [[9](#)]. The sludge formation also consequently influences the carbide content, carbon particles dispersion, bath superheat and loss of current efficiency. Extensive sludge formation increases the occurrence of anode effect, during which the anode is poorly wetted by the electrolyte resulting in extensive carbon dusting. Presence of dispersed carbon particles in the bath not only increases the electrical resistivity of the bath (i.e. higher energy consumption) [[10](#)], but also by reaction with dissolved aluminum and formation of aluminum carbide, causes higher solubility of aluminum and loss of current efficiency [[11](#), [12](#)].

Besides, the sludge also tampers with the hydrodynamics of the cell. The higher electrical resistivity of the sludge-covered cathode area diverts the local current to flow horizontally towards the edges of the sludge. Such horizontal current flows perturb the dominant vertical current flows leading to additional instability of the metal-bath interface. The oscillation of metal-bath interface has a dramatic effect on the optimum operation of the cell considering the large aspect ratio of the cell and higher resistivity of the bath compared to metal pad [[13](#)]. Moreover, the shear amount of metal-bath interfacial stress leads to higher aluminum solubility (i.e. fogging effect), which consecutively accounts for higher back reaction and loss of current efficiency [[14](#): p. 216-226]. In addition, such metal/bath instabilities results in an increase of anode-cathode distance (ACD), cathode voltage drop (CVD) and disturb heat balance which dramatically affect the current efficiency and energy consumption [[15](#)].

3. Thermochemistry of Sludge Phase

Thermodynamics of the metallurgical systems is of great importance since it can guide the scientists to not only find the optimum pressure, temperature and compositions but also it provides an in depth study of the interactions that happen between the cell's fluids, linings, cathode materials and impurities. The review of such systems is way out of the scope of this concise review article but avid readers are referred to references such as [Thonstad et al. \[14\]](#) and [Sorlie and Øye \[16\]](#). To our best of knowledge, the most exhaustive and specific thermodynamic study of the sludge in the aluminum electrolysis cells has been done partially by [Liu \[17\]](#) and more comprehensively by [Allard et al. \[5\]](#).

The main points according to Liu [17] could be summarized as follows: first, the dissolution of the bottom crust also known as ridge is hindered due to its insulating effect. As it is mentioned, when the cell is heated up to dissolve the cathodic deposits, this process may take few days. The reason for the delay can be partly attributed to the high temperature gradient within the cathodic deposits (5 – 10 °C), called insulating effect of the cathodic deposits. Second, the difference in liquidus temperatures of various sludge samples (950-964 °C) is mostly due to the CaF₂ content since excess AlF₃ has little impact on liquidus curve in the range of 0-7%. According to Allard et al. [5], the main chemical species of sludge samples found in industrial cells are Na₃AlF₆, Na₅Al₃F₁₄, Na₂Ca₃Al₂F₁₄ and α-alumina. As long as the bath is not supersaturated with alumina, addition of alumina decreases the liquidus temperature. However, as the concentration of alumina goes beyond 7 %, the liquidus temperature starts to rise. The melting temperature of the solid solution phase (cryolite + CaF₂ + AlF₃) is highly influenced by alumina content as long as it is less than 7%, while at higher alumina content, an isothermal melting point of 933 °C is noticed. The typical concentration of CaF₂ in deposits is 2 - 5 %. Based on experimental results, most of the calcium content within the deposits comes from Na₂Ca₃Al₂F₁₄ and NaCaAlF₆. NaCaAlF₆ can form a solid solution in α/β-cryolite. High CaF₂ content decreases the sludge solubility. Other solid calcium containing phases include Na₂Ca₃Al₂F₁₄ (formed at CaF₂ % > 10 %) and Na₄Ca₄Al₇F₃₃ (formed at high acidity). The sludge (typically containing 40 % alumina), may behave as a mixture of solid alumina in a liquid (at T > 933 °C) or, if heat losses are high enough as a solid phase (at T < 933 °C). In conclusion, the temperature of the cell's bottom must be kept well above 951 °C in order to keep the liquid fraction of the sludge around 70 % and enhance the possibility of the sludge dissolution. [5]

4. Important Factors in Sludge Formation/Dissolution

Formation/dissolution of sludge or resistive central cathodic deposits in aluminum electrolysis cells is correlated to several parameters such as cell's hydrodynamics, operational temperature, bath chemistry, physicochemical characteristics of alumina and feeding strategies.

4.1. Hydrodynamics

One of the strongest source of agitation in the electrolysis cells is the magneto-hydrodynamics (MHD) force. Such a force is the result of the interaction between the high-amperage DC electrical current and the magnetic field created by this current. It has to be emphasized that the shearing stress at the interface of metal/bath leads to excessive dissolution of aluminum (i.e. fogging effect) and such aluminum species leads to excessive formation of carbide within the cells and further loss of current efficiency [14, p. 216-226]. In order to minimize the detrimental effect of MHD forces, a typical layer of 25 cm of molten aluminum is maintained during the operation [4].

However, since the metal pad moves mostly under the influence of electromagnetic force field, such movements may also help the back-feeding of sludge. Sludge dissolution is a long and time consuming process since it is not in direct contact with the bulk bath. Thonstad, Johansen and Kristensen [18] mention that dissolution rate of sludge is approximately independent of agitation rate and diffusion controlled. On the other hand, comparing the dissolution rate of alumina particles in the industrial cells, it has been revealed that bubble induced agitation of the bath is also of great importance [14, p. 308]. As it is introduced in the alumina feeding strategies (Section 4.3), the diversion of anodic bubbles towards the feeding channel has enhanced the alumina dissolution.

4.2. Temperature

Due to the multicomponent nature of the bath and its consequences on the phase diagram, operational temperature is also related to the superheat level of the bath. The operating temperature of the modern aluminum smelters depends on the acidity of the bath and superheat level (Figure 1). The dissolution reaction of alumina is an endothermic process, moreover the alumina feed is at room temperature. The summation of the dissolution energy and sensible heat is enough to decrease the temperature of the melt by 15 °C if 1 wt% of alumina (with respect to total mass of the bath) is introduced into the cell [15]. Such calculations show that heat transfer within the cell is crucial for proper dissolution of the alumina and further prevention of sludge formation. Moreover, [Hove and Kvande \[19\]](#) have shown that higher temperatures enhance the back-feeding of sludge. It has been well established that proper heat transfer to the alumina particles in the feeding zone is crucial for avoiding sludge formation. The preheating of the alumina particles (600 °C) for compensation of the sensible heat, has been quite effective in increasing the dissolution rate of the alumina particles (+ 80 %) but, it has shown negative effect on dissolution rate of alumina agglomerates (- 30 %) [20]. It is claimed that the negative or negligible effect of preheating on dissolution rate of alumina agglomerates is related to the loss of moisture content [20]. The most effective parameter for the dissolution of the alumina agglomerates is the superheat level. It has been shown that a 20 °C increase of superheat level from 10 °C to 30 °C may enhance the dissolution rate of the alumina agglomerates up to 50 % [20]. On the other side, lower superheat level can reduce the dissolution rate of the alumina agglomerates up to 35 - 50 % [21].

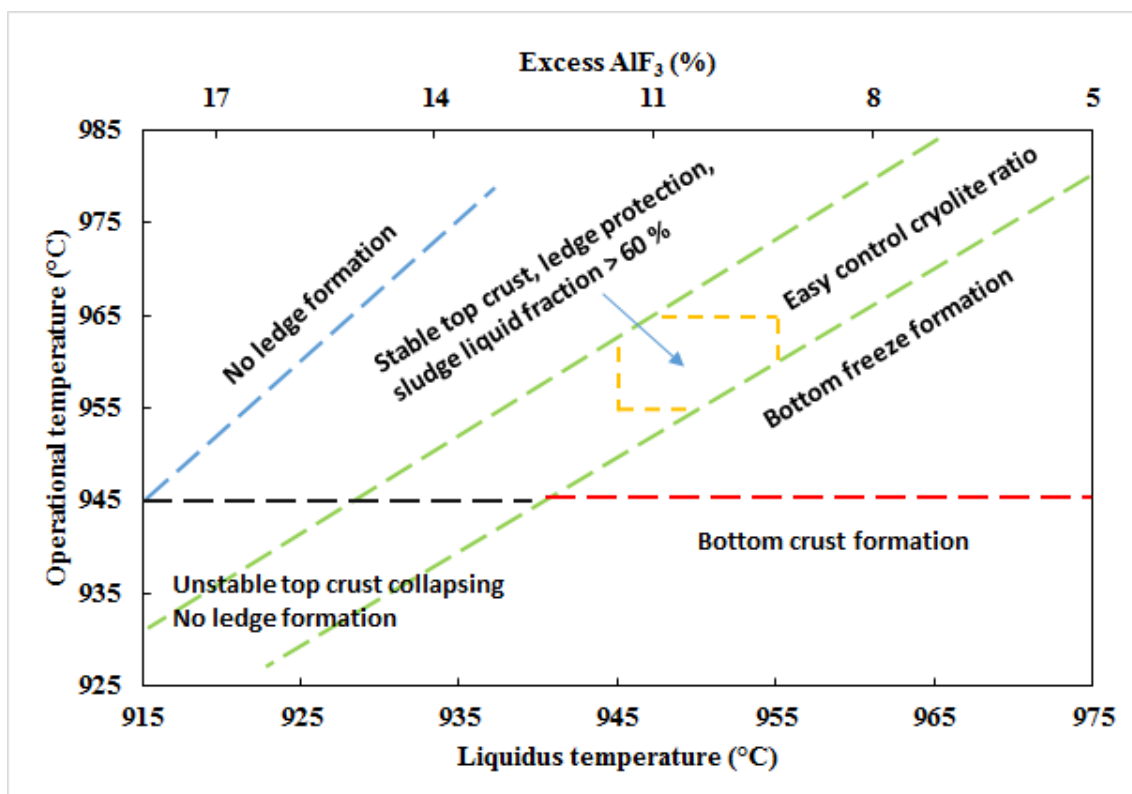


Figure 1. The schematic influence of temperature and bath acidity on operation of the cells; adapted from [Taylor and Welch \[22\]](#) and [Allard et al. \[5\]](#).

[Coulombe et al. \[23\]](#) have investigated the influence of the heat transfer rate on sludge formation in laboratory scale setup. It has been shown that more sludge is formed at lower heat transfer rate from the walls of an experimental cell, when compared to tests with higher heat

transfer rate. They justify such results by claiming that for tests with higher heat transfer rate, more cryolite is precipitated and an extended ledge toe is formed. Such ledge toe extension links to the sludge and creates a less dense liquid (compared to aluminum) with lower liquidus temperature, which in turn helps the dissolution of the sludge. The influence of proper heat transfer in avoiding the formation of alumina agglomerate/sludge or enhancing its dissolution is linked to proper turbulence of the bath at feeding zone.

4.3. Physico-chemical characteristics of alumina and alumina feeding strategy

Tabereaux and Peterson [4] have summarized some of the most important characteristics of alumina feed. Such factors include angle of repose of 33 - 35 °C, attrition index of 10 – 15 %, fines ($\leq 45 \mu\text{m}$) in fraction of 6 - 8%, superfines ($\leq 20 \mu\text{m}$) in fraction of 0.5 - 3 %, α -alumina content of 2 - 15 %, moisture content of 0.65 - 0.90, % loss on ignition, surface area (BET) 60 – 80 m^2/g , loose density of 0.96 g/cm^3 and a vibrated bulk density of 1.1 g/cm^3 . Besides, the saturation concentration of alumina in the bath (i.e., NaF-AlF₃-CaF₂-alumina system) is around 7 - 8 % depending on the acidity of the bath in the range of 6 - 16 % AlF₃.

As Grjotheim and Kvande [6: p 66-67] indicate, the normal grain size of the alumina feed is 20 - 150 μm . Big particles do not dissolve properly within bath while fine particles create fume emission and difficulty in mechanical handling. Coarse particles ($\geq 100 \mu\text{m}$) fraction is usually < 15 % (preferably 2 - 7 %) whereas fine particles ($\leq 45 \mu\text{m}$) fraction is usually < 20 % (preferably 3 - 8 %). Superfine particles ($\leq 20 \mu\text{m}$) fraction is also very important and its preferential content is approximately 0.5 %. Finer particles create top crusts with shorter life time, yet the density of the crusts will be higher than the ones made from coarse particles [24]. Fine particles dissolve individually faster than coarse particles but the poor wetting properties of fine particles as bulk lead to a slower dissolution [25]. Due to such poor wetting properties, electrolyte cannot penetrate within the intergranular voids and instead, finer particles fill the voids between the coarser particles and the rafts float for a much longer time before dissolving [25]. Moreover, fine particles contain larger amount of α -alumina compared to the bulk of the feed alumina which also causes a hard-to-dissolve top-crust/raft/agglomerates [26]. On the other hand, it has been claimed that there is no correlation between the size of the alumina particles (or median size) and dissolution rate [27, 28]. Wang [29] has categorized some of the different results on the influence of alumina particle size on the dissolution rate.

The porosity of primary alumina is in general around 75 % and it does not have any significant influence on the dissolution behaviour [6, p. 67]. As it is mentioned in section 4.2, the preheating of alumina to low temperatures (100 – 300 °C) has a detrimental effect on the dissolution rate of alumina. This phenomenon is related to the loss on ignition (LOI) [20]. The volatile content of the alumina not only causes more turbulence by eruptive behaviour of evolved gases, but also reduces the flow funnel time of the alumina particles, leading to better dispersion and enhanced mass/heat transfer [15]. According to Wang [29], there are different research results pertaining to the effect of surface area on alumina particles' dissolution rate. Some results indicate that higher surface area enhances the dissolution rate [27] whereas some other mention that surface area has negligible effect on the dissolution rate [30]. Nevertheless, there is a strong relationship between the LOI and the specific surface area of alumina particles [31]. Some of the researches show that higher α -alumina content and coarser particles tend to increase the dissolution rate while some other researches show that there is no correlation between the particle size distribution and the dissolution rate [29]. Such contradictory results may be due to the numerous factors that affect the alumina dissolution such as the physical, chemical, morphological and microstructural traits of fed alumina, as well as the dynamics of the feeding process, the chemistry of the electrolyte, and the superheat level of the bath [4].

Smelting grade alumina (SGA) typically consists mostly of γ -alumina (also known as sandy alumina) with a 2 – 15 % of α -alumina (also known as floury alumina) [4]. The type point fed alumina is important since γ -alumina has a lower flow funnel time, higher surface area and higher dissolution rate which makes it more ideal for aluminum electrolysis cells. Upon addition to the melt, γ -alumina exothermally transforms into α -alumina, which is less soluble, and later, endothermally dissolves within the bath. γ -alumina transformation into α -alumina creates thin plates (approximately 0.5 μm) while thicker alumina plates (approximately 1.5 μm) are the initial feed α -alumina content that has precipitated without dissolution and act as building blocks of the agglomerates [14, p. 296]. Also it has to be emphasized that as time goes on and with the aid of heat loss, the alumina platelets within the sludge start to grow by crystallization of alumina-saturated interstitial bath of the agglomerates [32].

According to Hove and Kvande [19], there is a direct relationship between the feeding strategy, anode effect and sludge formation. It means that the state of sludge formation is related to the volume of the batch of fed alumina, rate of the feeding and duration of feeding time. For example, in the worst case scenario, a huge volume of alumina fed at high rate and short duration of time may increase the sludge formation and leads to anode effect. One of the most significant inventions in the Hall-Héroult process was the introduction of point feeders in the 1960s in USA [33]. Point feeders use 2 - 6 holes (punched by 6-10 cm rods) through the top-crust to administer approximately 1 - 5 kg of alumina per each feeder pipe per one minute or so [33, 34]. Such an approach simultaneously minimizes the sludge formation and dusts/fluorides emission and has led to anode effect frequency of less than 0.02 per pot per day [22].

Nevertheless, point feeders have their own drawbacks. One of the drawbacks of push-feeding is the fluctuation of the alumina content as the crust breaker can't introduce all the feed that hopper has added [20]. The crust breaker is used to push-feed the alumina into the bath when the feeding holes are closed by piled-up alumina [34]. The piled-up alumina is prone to get sintered into α -alumina and particles' clotting [20], which not only hinder the alumina dissolution process but also increase the possibility of sludge formation. So, one of the most important factors in avoiding the formation of sludge is to keep the feeding holes open. In order to do so, one approach is to increase the bath turbulence and dissolution rate of the fed alumina by diverting the anodic gases towards the feeding zone [35]. Finally, some improvements of feeding pipe design and increasing the delivery height of the feed release has been practiced to not only reduce the feeding rate of the alumina but also increase the penetration depth of the alumina particles into the bath [36, 37].

4.4. Bath Chemistry

The chemistry of the bath is a significant parameter in the normal operation of the electrolysis cells and as it is well established it is interlinked with the current efficiency and environmental issues [38]. Among the 10 most important breakthroughs and developments in industrial aluminium process, three distinct parameters are directly related to the chemistry of the bath, namely point feeding technology, computer controlling of the cell and higher AlF_3 bath chemistry [33]. The point feeding technology tries to create a low level of alumina content (1-5 %) while using the line amperage and cell's resistivity as a method to monitor alumina content. Higher acidity of the bath was first tried in 1950s and when it showed potentials for improvement of current efficiency, it became a cornerstone of next generations of the cells [39].

A typical electrolysis cell uses 9 - 11 % AlF_3 , 4 - 6 % CaF_2 , 1.5 - 4 % Al_2O_3 and in some cases 2 - 4 % MgF_2 or LiF [4]. The application of LiF and MgF_2 is to reduce the aluminium solubility in the bath and hence increase the current efficiency [40]. It has been shown that with the addition of LiF (2 - 4 %) or AlF_3 (10 %), no significant change in the pattern of bottom crust formation is noticed; however, industrial tests have shown that the usage of lithium fluoride or low cryolite

ratios exacerbates the bottom crust formation [41]. A summary of the effects of various additives on the physicochemical properties of the bath has been presented by Habashi [42]. Moreover, the influence of impurities such as silica and iron oxide is reviewed by other references [14, 43].

All of the common additives (i.e. LiF, NaF, CaF₂, MgF₂ and AlF₃) reduce the liquidus temperature of the bath [44]. The reduction of liquidus temperature is a beneficial phenomenon since it reduces the operating temperature and enhances the current efficiency [40]. This is also beneficial since at constant operating temperature, lower liquidus temperature (i.e. higher superheat level), reduces the chance of sludge solidification. On the other hand, almost all the aforementioned common additives reduce the solubility of alumina which enhances the possibility of sludge formation.

The chemistry of the bath also defines the viscosity and density of the bath which are among the parameters that affect the current efficiency [45]. Lower density of the bath consequently reduces the density of the alumina-bath agglomerates, hence hindering the sludge formation [46]. Since the density of aluminum pad (2300 kg/m³) does not change significantly with temperature within the range of 940 - 970 °C, most of the density difference is accounted for by the cryolitic melt. Preferably a density difference > 200 kg/m³ provides proper separation between the metallic and cryolitic melts [6: p. 53]. Besides, lower bath densities specially in the case of lithium containing systems can create carbon particles accumulation at the metal-bath interface (also known as carbonation) [47]. Presence of carbon particles in the system may lead to increased bath electrical resistivity and loss of current efficiency [43: p. 394]. In addition to density, viscosity of the electrolyte also affects the hydrodynamics of fluids influencing phenomena such as gas bubble detachment and precipitation of undissolved alumina agglomerates [44]. A high viscosity not only can reduce the transfer rate of dissolved aluminium leading to less back reaction and higher current efficiency [48], but also can reduce the terminal velocity of the alumina agglomerates.

After alumina particles agglomerate and sink through the bath, there is yet another barrier (i.e. interface of metal/melt) to cross before they reach to the surface of the cathode block. All common additives increase the metal/melt interfacial tension. Lower cryolite ratio and higher alumina content also increase the interfacial tension while the bath is not saturated with alumina [14: p. 105-108]. In addition to the aforementioned factors, evaporation of volatile species also affects the chemistry of the bath. The most volatile species are the sodium and aluminum fluoride or the combination of these species as NaAlF₄ [6: p. 57]. Evaporation of such chemicals changes the cryolite ratio and it is required to control the bath chemistry by introduction of fresh materials. High cryolite ratio increases the liquidus temperature and consequently the sludge finds more opportunity to transform into solid deposit [49].

4.5. Conclusion

Hall-Héroult process has gone through numerous adjustments since its commercialization at the end of 19th century. Such adjustments include modification of the bath chemistry, sophisticated control and feeding systems, application of novel refractory materials, development of new cathode materials, magnetic field compensation, optimization of anode effect frequency, etc. Such adjustments all had one aim and it was to increase the current efficiency. According to Welch [38], each of the former adjustments have increased the current efficiency up to 2 % and nowadays a current efficiency of ~ 96 % is practical [22]. But, if the aim of the aluminium industry is to reach current efficiency of 97 % by 2020 [50], better understanding of the phenomena that cause loss of current efficiency is necessary. Maybe one of the oldest and still existing problems of the aluminium smelters is the sludge formation. Presence of sludge dramatically reduces current efficiency by tampering with operational temperature, bath

chemistry, current density and stability of the metal-bath interface. This concise review article tries to provide a reminder on the existing problem of sludge formation (also known as muck) and hopes to motivate young scientists and engineers to pull the aluminum industry out of sludge!

5. References

1. E.L. Bray, Aluminum, *U.S. Geological Survey, Mineral Commodity Summaries*. (2016).
2. X. Zhang, et al., A Novel Aluminum–Graphite Dual-Ion Battery, *Advanced Energy Materials*. Vol. 6, No. 11, (2016), 1502588-n/a.
3. E.L. Bray, *U.S. Geological Survey, Minerals Yearbook*. 2017.
4. A.T. Tabereaux and R.D. Peterson, Aluminum Production, in *Treatise on Process Metallurgy*, Vol. 3, S. Seetharaman, Editor. 2014, Elsevier: Boston, MA, USA. 839-917.
5. F. Allard, et al., Thermodynamic and thermochemical investigation of the deposits formed on the cathode surface of aluminum electrolysis cells, *Journal of Thermal Analysis and Calorimetry*. Vol. 119, No. 2, (2015), 1303-1314.
6. K. Grjotheim and H. Kvande, Introduction to Aluminium Electrolysis: Understanding the Hall-Héroult Process. 1993, Düsseldorf, Germany: Aluminium-Verlag GmbH. 260.
7. R. Keller, Alumina dissolution and sludge formation revisited, in *Light Metals 2005*, 147-150.
8. P.-Y. Geay, B.J. Welch and P. Homsy, Sludge in operating aluminum smelting cells, *Light Metals 2001*, 541-547.
9. X. Liao and H.A. Øye, Carbon Cathode Corrosion by Aluminium Carbide Formation in Cryolitic Melts, in *Essential Readings in Light Metals*, Vol. 4, A. Tomsett and J. Johnson, Editors. 2013, John Wiley & Sons, Inc. 992-998, also in *Light Metals 1999*, 621-627.
10. L. Bugnion and J.C. Fischer, Effect of Carbon Dust on the Electrical Resistivity of Cryolite Bath, in *Light Metals 2016*, 587-591.
11. R. Odegård, A. Sterten, and J. Thonstad, On the Solubility of Aluminium Carbide in Cryolitic Melts - Influence on Cell Performance, in *Essential Readings in Light Metals*, Vol. 2, G. Bearne, M. Dupuis, and G. Tarcy, Editors. 2013, John Wiley and Sons Inc. 25-32, also in *Light Metals 1987*, 295-302.
12. L. Wang, A.T. Tabereaux, and N.E. Richards, Electrical conductivity of cryolitic melts containing aluminum carbide, in *Light metals 1994*, 177-185.
13. P.A. Davidson and R.I. Lindsay, Stability of interfacial waves in aluminium reduction cells, *Journal of Fluid Mechanics*. Vol. 362, (1998), 273-295.
14. J. Thonstad, et al., Aluminium electrolysis: fundamentals of the Hall-Héroult process. 3rd ed. 2001, Düsseldorf, Germany: Aluminium-Verlag. 359.
15. B.J. Welch and G.I. Kuschel, Crust and alumina powder dissolution in aluminum smelting electrolytes, *JOM*. Vol. 59, No. 5, (2007), 50-54.
16. M. Sorlie and H.A. Oye, Cathodes in Aluminium Electrolysis. 3rd ed. 2010, Düsseldorf, Germany: Aluminium Verlag GmbH. 662.
17. X. Liu, Thermochemistry of Electrolyte, Sludge/Ridge, Ledge and Cell Cover, in *Proceedings of the 5th Australasian Aluminum Smelter Technology Workshop*. 1995: Queenstown, New Zealand. 619-627.
18. J. Thonstad, P. Johansen, and E.W. Kristensen, Some properties of alumina sludge, in *Light Metals 1980*, 227-239.
19. S.J. Hove and H. Kvande, Center-break alumina feeding and sludge control of prebaked cells, in *Light Metals 1982*, 513-529.
20. O. Kobbeltvedt, Dissolution kinetics for alumina in cryolite melts. Distribution of alumina in the electrolyte of industrial aluminium cells. Thesis (Dr.ing.), Norwegian

- University of Science and Technology, Department of Electrochemistry, Trondheim, Norway, 1997, p191.
21. G.I. Kuschel and B.J. Welch, Further Studies of Alumina Dissolution Under Conditions Similar to Cell Operation, in *Essential Readings in Light Metals*, Vol. 2, G. Bearne, M. Dupuis, and G. Tarcy, Editors. 2013, John Wiley & Sons, Inc.: Hoboken, NJ, USA. 112-118.
 22. M.P. Taylor and B.J. Welch, The future outlook and challenges for smelting aluminium, *Aluminium International Today*. Vol. 16, No. 2, (2004), 20-24.
 23. M.-A. Coulombe, et al., Factors Leading to the Formation of a Resistive Thin Film at the Bottom of Aluminum Electrolysis Cells, *Metallurgical and Materials Transactions B*. Vol. 47, No. 2, (2016), 1280-1295.
 24. J. Gerlach and G. Winkhaus, Interactions of alumina with cryolite-based melts, in *Light Metals* 1985, 301-313.
 25. L.A. Isaeva, A.B. Braslavskii, and P.V. Polyakov, Effect of the content of the α -phase and granulometric composition on the dissolution rate of alumina in cryolite-alumina melts, *Russian Journal of Non-Ferrous Metals*. Vol. 50, No. 6, (2009), 600-605.
 26. J.B. Metson, M.M. Hyland, and T. Groutso, Alumina phase distribution, structural hydroxyl and performance of smelter grade aluminas in the reduction cell, in *Light Metals* 2005, 127-131.
 27. A.N. Bagshaw and B.J. Welch, The Influence of Alumina Properties on Its Dissolution in Smelting Electrolyte, in *Essential Readings in Light Metals*, Vol. 1, D. Donaldson and B.E. Raahauge, Editors. 2013, John Wiley & Sons, Inc.: Hoboken, NJ, USA. 783-787.
 28. H. Maeda, S. Matsui, and A. Era, Measurement of dissolution rate of alumina in cryolite melt, in *Light Metals* 1985, 763-780.
 29. X. Wang, Alumina dissolution in aluminum smelting electrolyte, in *Light Metals* 2009, 383-388.
 30. R.K. Jain, et al., Interaction of aluminas with aluminium smelting electrolytes, in *Light Metals* 1983, 609-622.
 31. J.P. McGeer and J.D. Zwicker, Alumina: Calcination Control and Smelting Use, *JOM*. Vol. 34, No. 5, (1982), 50-54.
 32. I.S. Kachanovskaya and O.I. Arakelyan, Behavior of alumina in the deposits and crust of an aluminum electrolytic cell, *Tsvetnye Metally*. No. 4, (1976), 37-40.
 33. G.P. Tarcy, H. Kvande, and A. Tabereaux, Advancing the industrial aluminum process: 20th century breakthrough inventions and developments, *JOM*. Vol. 63, No. 8, (2011), 101-108.
 34. P. Lavoie, M.P. Taylor, and J.B. Metson, A Review of Alumina Feeding and Dissolution Factors in Aluminum Reduction Cells, *Metallurgical and Materials Transactions B*. Vol. 47, No. 4, (2016), 2690-2696.
 35. B.P. Moxnes, B.E. Aga, and J.H. Skaar, How to obtain open feeder holes by installing anodes with tracks, in *Light Metals* 1998, 247-255.
 36. J. Tessier, et al., Improvement of Alumina Dissolution Rate through Alumina Feeder Pipe Modification, in *Light Metals* 2013, 711-717.
 37. A.N. Bagshaw, et al., Effect of operating conditions in the dissolution of primary and secondary (reacted) alumina powders in electrolytes, in *Light Metals* 1985, 649-659.
 38. B.J. Welch, Gaining That Extra 2 Percent Current Efficiency, in *Hall-Héroult Centennial*, W.S. Peterson and R.E. Miller, Editors. 2007, John Wiley & Sons, Inc.: Hoboken, NJ, USA. 120-129.
 39. G.T. Holmes, Hall cell ampere efficiency up 12% in 3 decades, in *Light Metals* 1995, 371-373.
 40. E. Rosshard, et al., EPT 18: the new 180-kA-pot of Alusuisse, in *Light Metals* 1983, 595-605.

41. J. Thonstad, S. Roenning, and P. Entner, Formation of bottom crusts in aluminum pots. A laboratory study, in *Light Metals* 1982, 485-97.
42. F. Habashi, Extractive Metallurgy of Aluminum, in *Handbook of Aluminum*, Vol. 2, G.E. Totten and D.S. MacKenzie, Editors. 2003, Marcel Dekker: NY, USA. 1-79.
43. K. Grjotheim, et al., Aluminium electrolysis: fundamentals of the Hall-Héroult process. 2nd ed. 1982, Düsseldorf, Germany: Aluminium-Verlag. 443.
44. W. Haupin, The influence of additives on Hall-Héroult bath properties, *JOM*. Vol. 43, No. 11, (1991), 28-34.
45. K. Grjotheim, W.E. Haupin, and B.J. Welch, Current efficiency - relating fundamental studies to practice, in *Light Metals* 1985, 679-694.
46. R. Keller, Alumina dissolution and sludge formation, in *Light Metals* 1984, 513-518.
47. P. Coursol, et al., Application of Thermodynamic Models for Better Understanding and Optimizing the Hall-Heroult Process, *JOM*. Vol. 64, No. 11, (2012), 1326-1333.
48. C. Robelin and P. Chartrand, A viscosity model for the (NaF + AlF₃ + CaF₂ + Al₂O₃) electrolyte, *The Journal of Chemical Thermodynamics*. Vol. 43, No. 5, (2011), 764-774.
49. F. Allard, et al., Cartography and chemical composition of the different deposits in the hall-heroult process, in *Light Metals* 2014, 1233-1238.
50. H. Kvande, Production of primary aluminium, in *Fundamentals of Aluminium Metallurgy: Production, processing and applications*, R. Lumley, Editor. 2011, Woodhead Publishing: Cambridge, UK. 49-69.